Spectrum of Engineering Sciences
ISSN (e) 3007-3138 (p) 3007-312X Volume 4, Issue 5, 2026

DEGREE-BASED TOPOLOGICAL INDICES AND QSPR MODELING OF SELECTED COVID-19 CANDIDATE DRUGS

Kousar Perveen[1], Muazzam Ali[*2], M U Hashmi[3], Affan Ahmad[4]

[1]*Department of Basic Sciences, Superior University, Lahore*
[*2,3,4]*Department of Computer Science, Superior University, Lahore*

[*2]muazzamali@superior.edu.pk

DOI: https://doi.org/10.5281/zenodo.20302968

Keywords
Topological indices, QSPR analysis, antiviral drugs, COVID-19 treatment, drug discovery, degree-based descriptors

Article History
Received: 11 March 2026
Accepted: 21 April 2026
Published: 20 May 2026

Corresponding Author: *
Muazzam Ali

Abstract
This research have considered structural and physicochemical significance of various degree-based topological indices for Remdesivir, Chloroquine, Hydroxychloroquine, Theaflavin, Ritonavir, and Arbidol, both antiviral and COVID-19 related, candidate drugs. Edge structures of the compounds were created and then analyzed using edge partitioning for vertex degrees of these compounds. Six different indices based on the degrees were considered: the Quadratic-Contraharmonic Index, the Contraharmonic-Quadratic Index, Geometric Quadratic Index, Quadratic Geometric Index, Arithmetic-Contraharmonic Index, and Contraharmonic-Arithmetic Index. In the calculated values, Ritonavir gives highest values in all values which means that it is more structurally complex and has more important molecular descriptors associated with its structure and more important, Remdesivir and Theaflavin were the next highest values. Arbidol yielded moderate index values whereas, Chloroquine and Hydroxychloroquine yielded comparatively lower index values. The predictive value of these descriptors was tested by correlating the topological indices with physicochemical properties such as boiling point, enthalpy of vaporization, flash point, molar refractivity, polar surface area, polarizability, surface tension and molar volume. The correlation analysis showed very high positive correlation between the proposed indices and several properties especially the boiling point, enthalpy of vaporization, polar surface area, molar refractivity and polarizability. There were weaker correlations between surface tension and moderate ones for molar volume. Such results indicate that the chosen topological indices could be helpful mathematical descriptors for the calculation of a set of important physicochemical properties for antiviral drugs, and as input for the computational screening process.

INTRODUCTION

Quantitative structure property relationship (QSPR) is a quantitative method that links the molecular framework of compounds with their physio-chemical or biological characteristics [6]. It allows for point-compound testing without the use of extensive equipment, predicting properties such as solubility, toxicity, and bioavailability, making drug development safer [7]. In diseases like COVID-19, early discovery of therapeutic agents is important, offering potential antiviral

compounds for treatment, reducing the time required for synthesis and testing. Topological indices have been understudied in drug discovery, especially in the context of the COVID-19 virus. Studies have shown correlations between topological indices and the biological activity of many drugs, including remdesivir, chloroquine, hydroxychloroquine, theaflavin, ritonavir, and arbidol [8,9]. These studies have shown that indices do exist correlations between the topological indices and the biological activity of these compounds, highlighting the importance of indices in drug designing.

The use of topological indices has been understudied in the context of drug discovery especially in the case of the COVID-19 virus. Scientific publications such as Syed Ajaz K. Kirmani et al. [1], Kansal et al. [9], and other similar papers have applied its topological indices and QSPR to predict physicochemical properties, in addition to the influence of antiviral effects, of many drugs, including remdesivir, chloroquine, hydroxychloroquine, theaflavin, ritonavir These studies have shown that indices do exist correlations between the topological indices and the biological activity of these compounds hence the importance of the indices in drug designing. For example, Kirmani et al. [1] studied the predictive power of degree-based topological indices using biological activity of antiviral drugs under consideration In, COVID-19 treatment, while Kansal et al. (2022) involved temperature - based topological indices for using in QSPR analysis in COVID-19 drugs.

In this paper, degree-based topological descriptors were calculated for several antiviral compounds, including remdesivir, chloroquine, hydroxychloroquine, theaflavin, ritonavir, and arbidol. QSPR analysis was considered to determine the relation between these evaluated indices and the physicochemical characteristics of all given drugs. The goal was to gain a better understanding of the inherent structural properties of these compounds and determine whether there are topological features directly linked to their antiviral action.

2. Methodology

In this study, we focus on several degree-based topological indices to evaluate the structural properties of antiviral drugs and their molecular graphs. Degree-based topological indices, such as the Quadratic-Contraharmonic Index (QCI) and Contraharmonic-Quadratic Index (CQI), are used to analyze molecular graphs of antiviral drugs for COVID-19 treatment. These indices quantify molecular characteristics and correlate with biological and chemical properties. They are useful in drug discovery, aiding in screening and selecting promising candidates for further testing. Combining these indices with QSPR analysis provides a comprehensive understanding of antiviral drugs' molecular characteristics and potential efficacy. The following indices have been selected for their relevance in capturing molecular characteristics and their ability to correlate with various physicochemical and biological properties.

2.1 Quadratic-Contraharmonic Indices

Quadratic-Contraharmonic indices are used in graph theory to study network morphology and connectedness, reflecting local and global features of nodes [10].

$$\mathrm{QCI}(\zeta) = \sum \frac{\mathrm{ds} + \mathrm{dt}}{\sqrt{2((\mathrm{ds})^2 + (\mathrm{dt})^2)}} \tag{1}$$

2.2 Contraharmonic-Quadratic Indices

Contraharmonic-Quadratic Indices (CQIs) are mathematical tools used in graph theory to analyze network structures, providing insights into node connectivity and facet distribution, and are used in fields like chemistry, biology, and communication networks [10].

$$\mathrm{CQI}(\zeta) = \sum \frac{\sqrt{2((\mathrm{ds})^2 + (\mathrm{dt})^2)}}{\mathrm{ds} + \mathrm{dt}} \tag{2}$$

2.3 Geometric Quadratic Index

The Geometric Quadratic Index is a topological index in graph theory that examines the structural capabilities of networks or molecular graphs by analyzing the relationships between neighboring vertices [11]. For a graph ζ, define its Geometric Quadratic Index as

$$GQI(\zeta) = \sum \sqrt{\frac{2dsdt}{ds^2 + dt^2}} \tag{3}$$

2.4 Quadratic Geometric Index

The Quadratic Geometric Index is a topological degree in graph theory that evaluates network and molecular graph structural properties by combining quadratic and geometric vertex levels, primarily used in chemistry and biology for predicting molecular houses [11].

$$QGI(\zeta) = \sum \sqrt{\frac{ds^2 + dt^2}{2dsdt}} \tag{4}$$

2.5 Arithmetic-Contraharmonic Index

The Arithmetic-Contraharmonic Index is a topological graph theory index that evaluates network and molecular graph structural traits using mathematics and contra harmonic vertex degrees. It's useful in chemistry, biology, and social network evaluation for predicting molecular homes [12].

$$\mathrm{ACI}(\zeta) = \sum \frac{(\mathrm{ds} + \mathrm{dt})^2}{2((\mathrm{ds})^2 + (\mathrm{dt})^2)} \tag{5}$$

2.6 Contraharmonic-Arithmetic Index

The Contraharmonic-Arithmetic indicator is a topological indicator in graph theory that evaluates network and molecular graph properties, providing a comprehensive representation of node connectivity and interactions, useful for predicting molecular homes and assessing complex systems [12].

$$\mathrm{CAI}(\zeta) = \sum \frac{2((\mathrm{ds})^2 + (\mathrm{dt})^2)}{(\mathrm{ds} + \mathrm{dt})^2} \tag{6}$$

2.7 Edge Partitioning Based on Degree

The study uses degree-based edge partitioning to classify antiviral drugs' molecular graphs into different categories. This method reveals structural trends and high-degree nodes, revealing the stability and robustness of molecular systems. Edge partitioning is useful for optimizing network performance, studying community structures, and detecting key relationships in complex systems [13]. It helps in drug discovery by examining how connectivity patterns influence biological activity, stability, and reactivity, aiding in the identification of compounds with optimal therapeutic potential for COVID-19 treatment.

Degree-based edge partitioning that groups edges of a graph based on the degrees of their connecting vertices, revealing distinct structural properties and connectivity trends within these subgraphs [14-16]. This method allows detecting nodes of high degree that are important in the connections within a network and provides information on how edge distribution impact global logographic behavior. Applications include the optimization of network performance and clustering algorithms, for community detection in social and biological networks via targeted relationship analysis to identify critical edge implementation that drives network stability.

(a) Remdesivir (GS-5734)

Remdesivir (GS-5734) is a nucleotide analog prodrug that become to begin with advanced to treat Ebola but gained prominence for the duration of the COVID-19 pandemic as an antiviral agent. It works by way of inhibiting the viral RNA-dependent RNA polymerase, which is critical for viral replication.

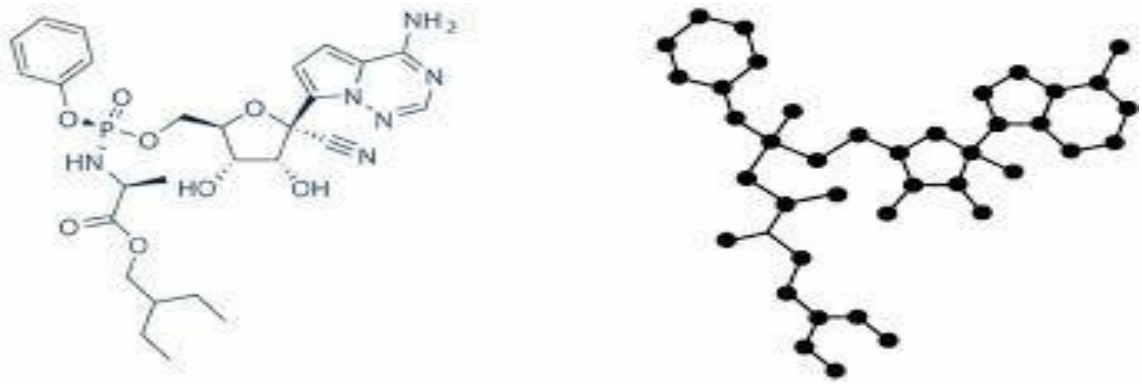

Figure 1. Structure of Remdesivir

Table 1: Edge partitioning of Remdesivir

($d_2(s)$, $d_2(t)$)	(1,2)	(1,3)	(1,4)	(2,2)	(2,3)	(2,4)	(3,3)	(3,4)	(3,6)	(3,7)
Frequency	2	5	2	9	14	6	6	2	3	1
($d_2(s)$, $d_2(t)$)	(3,8)	(4,4)	(4,5)	(4,6)	(4,7)	(4,9)	(5,5)	(5,6)	(5,7)	(5,8)
Frequency	1	2	4	2	1	1	2	6	1	2
($d_2(s)$, $d_2(t)$)	(5,9)	(6,6)	(6,7)	(6,8)	(7,7)	(7,8)	(7,9)	(8,8)	(8,9)	(9,9)
Frequency	1	1	3	1	4	1	1	1	2	1

(b) Chloroquine

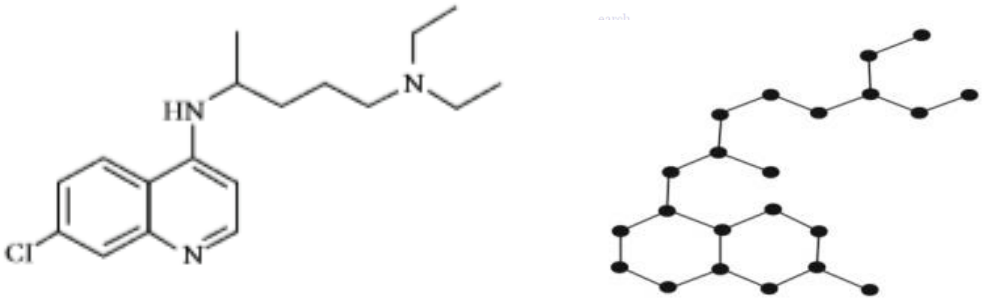

Figure 2: Chloroquine 's molecular graph

Malaria is treated with chloroquine. Early in the pandemic, it was investigated as a treatment for COVID-19, but research on this usage was mostly abandoned in the summer of 2020, and it is no longer advised. It is consumed orally. Figure 2 displays the chloroquine's molecular graph. This structure has 21 vertices and 23 edges.

Table 2: Edge partitioning of Chloroquine

($d_2(s)$, $d_2(t)$)	(1,2)	(1,3)	(2,2)	(2,3)	(3,3)	(2,4)	(3,5)	(4,5)	(4,6)
Frequency	2	2	5	12	2	2	2	4	2
($d_2(s)$, $d_2(t)$)	(5,5)	(5,6)	(5,7)	(5,8)	(6,7)	(7,8)			
Frequency	3	3	2	1	2	2			

(c) Hydroxychloroquine

Hydroxychloroquine is an antimalarial medication administered in regions where chloroquine- Sensitive malaria persists. Figure 3 displays hydroxychloroquine molecular graph. This structure has 22 vertices and 24 edges.

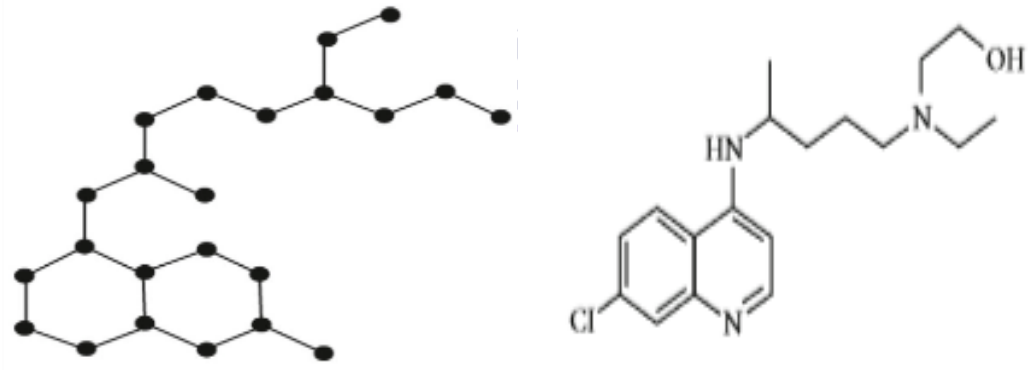

Figure 3 : Hydroxychloroquine 's molecular graph

Table 3: Edge partitioning of Hydroxychloroquine

($d_2(s)$, $d_2(t)$)	(1,2)	(1,3)	(2,2)	(2,3)	(3,3)	(2,4)	(3,5)	(4,5)
Frequency	2	2	6	13	2	1	3	4
($d_2(s)$, $d_2(t)$)	(4,6)	(5,5)	(5,6)	(5,7)	(5,8)	(6,7)	(7,8)	
Frequency	1	3	4	2	1	2	2	

(d) Theaflavin

A polyphenolic compound found in black tea, has potential antiviral, antioxidant, and anti-inflammatory properties.

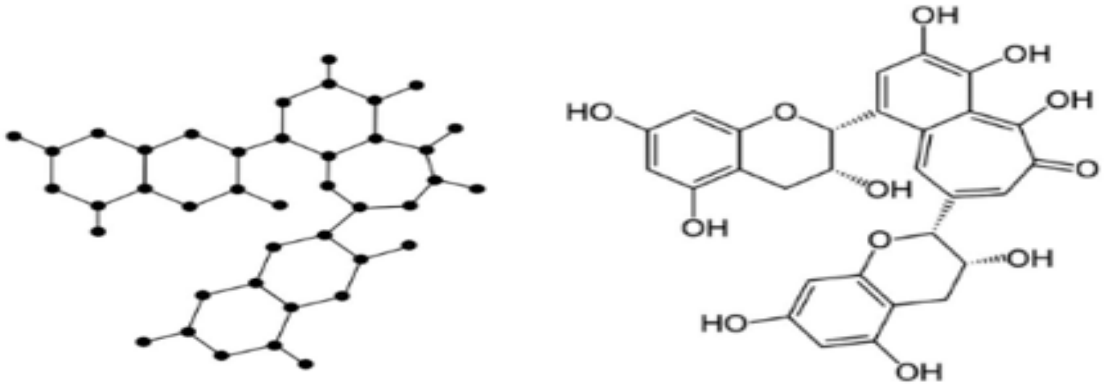

Figure 4: Theaflavin 's molecular graph

Table 4: Edge partitioning of theaflavin

($d_2(s)$, $d_2(t)$)	(1,3)	(2,3)	(3,3)	(3,5)	(3,6)	(3,7)	(5,6)
Frequency	10	22	14	2	6	2	4
($d_2(s)$, $d_2(t)$)	(6,6)	(6,7)	(6,8)	(7,8)	(7,9)	(8,8)	(8,9)
Frequency	6	8	10	3	2	2	1

(e) Ritonavir

A bioactive protein inhibitor medication called ritonavir is used to treat viruses. It produces noninfectious viruses by causing deregulation in the structure and functional proteins of the virus. Figure 5 displays ritonavir's molecular graph. This structure has 50 vertices and 53 edges.

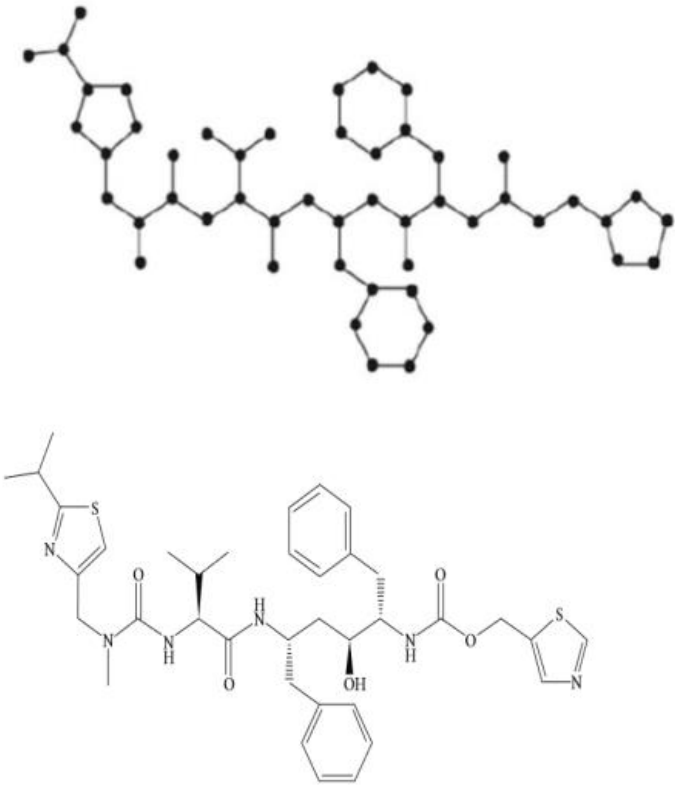

Figure-5 : Ritonavir 's molecular graph

Table 5: Edge partitioning of Ritonavir

($d_2(s)$, $d_2(t)$)	(1,3)	(2,2)	(2,3)	(3,3)	(3,5)	(4,4)	(3,6)	(4,5)
Frequency	9	13	26	5	5	5	4	6
($d_2(s)$, $d_2(t)$)	(5,5)	(5,6)	(5,7)	(6,6)	(5,8)	(6,7)	(6,8)	
Frequency	3	10	3	11	1	3	2	

(f) Arbidol

Arbidol (Umifenovir) is an antiviral drug extensively utilized in Russia and China for the remedy and prevention of influenza and different breathing viral infections. It works with the aid of inhibiting viral fusion with host cell membranes, as a result stopping the entry of the virus into cells. During the COVID-19 pandemic, Figure 6 displays arbidol's molecular graph .This structure has 29 vertices and 31 edges.

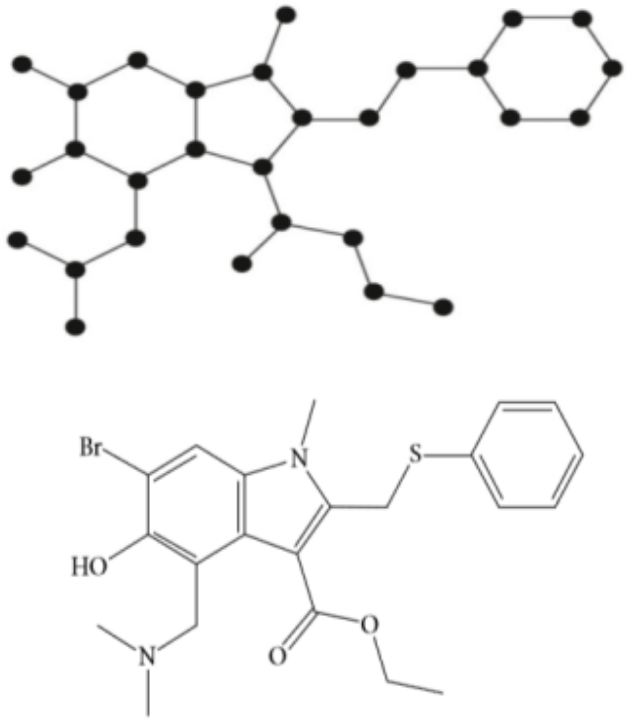

Figure. 6: Arbidol 's Molecular graph

Table 6: 4. RESULTS AND DISCUSSIONS

($d_2(s)$, $d_2(t)$)	(1,2)	(1,3)	(2,2)	(2,3)	(3,3)	(3,4)	(3,5)	(4,4)	(3,6)	(4,5)	(3,7)
Frequency	1	6	6	10	9	2	1	2	2	2	2
($d_2(s)$, $d_2(t)$)	(4,6)	(5,5)	(5,6)	(6,6)	(5,8)	(6,7)	(6,8)	(7,8)	(6,9)	(8,9)	(9,9)
Frequency	1	1	4	1	1	1	2	3	1	3	1

4.1 Results of Indices

In this sec, we calculate the main results Quadratic-Contraharmonic Index (QCI), Contra Harmonic-Quadratic Index (CQI), Geometric Quadratic Index (GQI), Quadratic Geometric Index (QGI), Arithmetic Contraharmonic Index (ACI) And Contraharmonic Arithmetic index (CAI) for Remdesivir, Chloroquine, Hydroxychloroquine, Theaflavin, Ritonavir, Arbidol. In the end, a comparison of the obtained results of the above indices and QSPR analysis is also presented.

Theorem 1. The Quadratic-Contraharmonic Index (QCI), Contra Harmonic-Quadratic Index (CQI), Geometric Quadratic Index (GQI), Quadratic Geometric Index (QGI), Arithmetic Contraharmonic Index (ACI) And Contraharmonic Arithmetic index (CAI) for Remdesivir are as follow

a) $NLQCI(\zeta) = 85.84$
b) $CQI(\zeta) = 90.24$
c) $GQI(\zeta) = 83.49$
d) $QGI(\zeta) = 93.40$
e) $ACI(\zeta) = 83.84$
f) $CAI(\zeta) = 92.84$

Proof. By using the degree-based edge partition of Table-1 and equations 1-6,

a) $QCI(\zeta) = \sum \frac{du+dv}{\sqrt{2((du)^2+(dv)^2)}} = \frac{1+2}{\sqrt{2((1)^2+(2)^2)}}(2) + \frac{1+3}{\sqrt{2((1)^2+(3)^2)}}(5) + \frac{1+4}{\sqrt{2((1)^2+(4)^2)}}(2)$
$+ \frac{2+2}{\sqrt{2((2)^2+(2)^2)}}(9) + \frac{2+3}{\sqrt{2((2)^2+(3)^2)}}(14) + \frac{2+4}{\sqrt{2((2)^2+(4)^2)}}(6) + \frac{3+3}{\sqrt{2((3)^2+(3)^2)}}(6) + \frac{3+4}{\sqrt{2((3)^2+(4)^2)}}(2) +$
$\frac{3+6}{\sqrt{2((3)^2+(6)^2)}}(3) + \frac{3+7}{\sqrt{2((3)^2+(7)^2)}}(1) + \frac{3+8}{\sqrt{2((3)^2+(8)^2)}}(1) + \frac{4+4}{\sqrt{2((4)^2+(4)^2)}}(2) + \frac{4+5}{\sqrt{2((4)^2+(5)^2)}}(4) +$
$\frac{4+6}{\sqrt{2((4)^2+(6)^2)}}(2) + \frac{4+7}{\sqrt{2((4)^2+(7)^2)}}(1) + \frac{4+9}{\sqrt{2((4)^2+(9)^2)}}(1) + \frac{5+5}{\sqrt{2((5)^2+(5)^2)}}(2) + \frac{5+6}{\sqrt{2((5)^2+(6)^2)}}(6) +$
$\frac{5+7}{\sqrt{2((5)^2+(7)^2)}}(1) + \frac{5+8}{\sqrt{2((5)^2+(8)^2)}}(2) + \frac{5+9}{\sqrt{2((5)^2+(9)^2)}}(1) + \frac{6+6}{\sqrt{2((6)^2+(6)^2)}}(1) + \frac{6+7}{\sqrt{2((6)^2+(7)^2)}}(3) +$
$\frac{6+8}{\sqrt{2((6)^2+(8)^2)}}(1) + \frac{7+7}{\sqrt{2((7)^2+(7)^2)}}(4) + \frac{7+8}{\sqrt{2((7)^2+(8)^2)}}(1) + \frac{7+9}{\sqrt{2((7)^2+(9)^2)}}(1) + \frac{8+8}{\sqrt{2((8)^2+(8)^2)}}(1) +$
$\frac{8+9}{\sqrt{2((8)^2+(9)^2)}}(2) + \frac{9+9}{\sqrt{2((9)^2+(9)^2)}}(1) = 85.84$

b) $CQI(\zeta) = \sum \frac{\sqrt{2((du)^2+(dv)^2)}}{du+dv} = \frac{\sqrt{2((1)^2+(2)^2)}}{1+2}(2) + \frac{\sqrt{2((1)^2+(3)^2)}}{1+3}(5) + \frac{\sqrt{2((1)^2+(4)^2)}}{1+4}(2)$
$+ \frac{\sqrt{2((2)^2+(2)^2)}}{2+2}(9) + \frac{\sqrt{2((2)^2+(3)^2)}}{2+3}(14) + \frac{\sqrt{2((2)^2+(4)^2)}}{2+4}(6) + \frac{\sqrt{2((3)^2+(3)^2)}}{3+3}(6) + \frac{\sqrt{2((3)^2+(4)^2)}}{3+4}(2) +$
$\frac{\sqrt{2((3)^2+(6)^2)}}{3+6}(3) + \frac{\sqrt{2((3)^2+(7)^2)}}{3+7}(1) + \frac{\sqrt{2((3)^2+(8)^2)}}{3+8}(1) + \frac{\sqrt{2((4)^2+(4)^2)}}{4+4}(2) + \frac{\sqrt{2((4)^2+(5)^2)}}{4+5}(4) +$
$\frac{\sqrt{2((4)^2+(6)^2)}}{4+6}(2) + \frac{\sqrt{2((4)^2+(7)^2)}}{4+7}(1) + \frac{\sqrt{2((4)^2+(9)^2)}}{4+9}(1) + \frac{\sqrt{2((5)^2+(5)^2)}}{5+5}(2) + \frac{\sqrt{2((5)^2+(6)^2)}}{5+6}(6) +$
$\frac{\sqrt{2((5)^2+(7)^2)}}{5+7}(1) + \frac{\sqrt{2((5)^2+(8)^2)}}{5+8}(2) + \frac{\sqrt{2((5)^2+(9)^2)}}{5+9}(1) + \frac{\sqrt{2((6)^2+(6)^2)}}{6+6}(1) + \frac{\sqrt{2((6)^2+(7)^2)}}{6+7}(3) +$
$\frac{\sqrt{2((6)^2+(8)^2)}}{6+8}(1) + \frac{\sqrt{2((7)^2+(7)^2)}}{7+7}(4) + \frac{\sqrt{2((7)^2+(8)^2)}}{7+8}(1) + \frac{\sqrt{2((7)^2+(9)^2)}}{7+9}(1) + \frac{\sqrt{2((8)^2+(8)^2)}}{8+8}(1) +$
$\frac{\sqrt{2((8)^2+(9)^2)}}{8+9}(2) + \frac{\sqrt{2((9)^2+(9)^2)}}{9+9}(1) = 90.24$

c) $GQI(\zeta) = \sum \sqrt{\frac{2dudv}{du^2+dv^2}} = \sqrt{\frac{2(1)(2)}{(1)^2+(2)^2}}(2) + \sqrt{\frac{2(1)(3)}{(1)^2+(3)^2}}(5) + \sqrt{\frac{2(1)(4)}{(1)^2+(4)^2}}(2) + \sqrt{\frac{2(2)(2)}{(2)^2+(2)^2}}(9) +$
$\sqrt{\frac{2(2)(3)}{(2)^2+(3)^2}}(14) + \sqrt{\frac{2(2)(4)}{(2)^2+(4)^2}}(6) + \sqrt{\frac{2(3)(3)}{(3)^2+(3)^2}}(6) + \sqrt{\frac{2(3)(4)}{(3)^2+(4)^2}}(2) + \sqrt{\frac{2(3)(6)}{(3)^2+(6)^2}}(3) + \sqrt{\frac{2(3)(7)}{(3)^2+(7)^2}}(1) +$
$\sqrt{\frac{2(3)(8)}{(3)^2+(8)^2}}(1) + \sqrt{\frac{2(4)(4)}{(4)^2+(4)^2}}(2) + \sqrt{\frac{2(4)(5)}{(4)^2+(5)^2}}(4) + \sqrt{\frac{2(4)(6)}{(4)^2+(6)^2}}(2) + \sqrt{\frac{2(4)(7)}{(4)^2+(7)^2}}(1) + \sqrt{\frac{2(4)(9)}{(4)^2+(9)^2}}(1) +$
$\sqrt{\frac{2(5)(5)}{(5)^2+(5)^2}}(2) + \sqrt{\frac{2(5)(6)}{(5)^2+(6)^2}}(6) + \sqrt{\frac{2(5)(7)}{(5)^2+(7)^2}}(1) + \sqrt{\frac{2(5)(8)}{(5)^2+(8)^2}}(2) + \sqrt{\frac{2(5)(9)}{(5)^2+(9)^2}}(1) + \sqrt{\frac{2(6)(6)}{(6)^2+(6)^2}}(1) +$
$\sqrt{\frac{2(6)(7)}{(6)^2+(7)^2}}(3) + \sqrt{\frac{2(6)(8)}{(6)^2+(8)^2}}(1) + \sqrt{\frac{2(7)(7)}{(7)^2+(7)^2}}(4) + \sqrt{\frac{2(7)(8)}{(7)^2+(8)^2}}(1) + \sqrt{\frac{2(7)(9)}{(7)^2+(9)^2}}(1) + \sqrt{\frac{2(8)(8)}{(8)^2+(8)^2}}(1) +$
$\sqrt{\frac{2(8)(9)}{(8)^2+(9)^2}}(2) + \sqrt{\frac{2(9)(9)}{(9)^2+(9)^2}}(1) = 83.49$

d) $QGI(\zeta) = \sum \sqrt{\frac{du^2+dv^2}{2dudv}} = \sqrt{\frac{(1)^2+(2)^2}{2(1)(2)}}(2) + \sqrt{\frac{(1)^2+(3)^2}{2(1)(3)}}(5) + \sqrt{\frac{(1)^2+(4)^2}{2(1)(4)}}(2) + \sqrt{\frac{(2)^2+(2)^2}{2(2)(2)}}(9)$
$+ \sqrt{\frac{(2)^2+(3)^2}{2(2)(3)}}(14) + \sqrt{\frac{(2)^2+(4)^2}{2(2)(4)}}(6) + \sqrt{\frac{(3)^2+(3)^2}{2(3)(3)}}(6) + \sqrt{\frac{(3)^2+(4)^2}{2(3)(4)}}(2) + \sqrt{\frac{(3)^2+(6)^2}{2(3)(6)}}(3) + \sqrt{\frac{(3)^2+(7)^2}{2(3)(7)}}(1) +$

$$\sqrt{\frac{(3)^2+(8)^2}{2(3)(8)}}(1)+\sqrt{\frac{(4)^2+(4)^2}{2(4)(4)}}(2)+\sqrt{\frac{(4)^2+(5)^2}{2(4)(5)}}(4)+\sqrt{\frac{(4)^2+(6)^2}{2(4)(6)}}(2)+\sqrt{\frac{(4)^2+(7)^2}{2(4)(7)}}(1)+\sqrt{\frac{(4)^2+(9)^2}{2(4)(9)}}(1)+$$
$$\sqrt{\frac{(5)^2+(5)^2}{2(5)(5)}}(2)+\sqrt{\frac{(5)^2+(6)^2}{2(5)(6)}}(6)+\sqrt{\frac{(5)^2+(7)^2}{2(5)(7)}}(1)+\sqrt{\frac{(5)^2+(8)^2}{2(5)(8)}}(2)+\sqrt{\frac{(5)^2+(9)^2}{2(5)(9)}}(1)+\sqrt{\frac{(6)^2+(6)^2}{2(6)(6)}}(1)+$$
$$\sqrt{\frac{(6)^2+(7)^2}{2(6)(7)}}(3)+\sqrt{\frac{(6)^2+(8)^2}{2(6)(8)}}(1)+\sqrt{\frac{(7)^2+(7)^2}{2(7)(7)}}(4)+\sqrt{\frac{(7)^2+(8)^2}{2(7)(8)}}(1)+\sqrt{\frac{(7)^2+(9)^2}{2(7)(9)}}(1)+\sqrt{\frac{(8)^2+(8)^2}{2(8)(8)}}(1)+$$
$$\sqrt{\frac{(8)^2+(9)^2}{2(8)(9)}}(2)+\sqrt{\frac{(9)^2+(9)^2}{2(9)(9)}}(1)=93.40$$

e) $$\mathrm{ACI}(\zeta)=\sum\frac{(du+dv)^2}{2((du)^2+(dv)^2)}=\frac{(1+2)^2}{2((1)^2+(2)^2)}(2)+\frac{(1+3)^2}{2((1)^2+(3)^2)}(5)+\frac{(1+4)^2}{2((1)^2+(4)^2)}(2)+\frac{(2+2)^2}{2((2)^2+(2)^2)}(9)+$$
$$\frac{(2+3)^2}{2((2)^2+(3)^2)}(14)+\frac{(2+4)^2}{2((2)^2+(4)^2)}(6)+\frac{(3+3)^2}{2((3)^2+(3)^2)}(6)+\frac{(3+4)^2}{2((3)^2+(4)^2)}(2)+\frac{(3+6)^2}{2((3)^2+(6)^2)}(3)+$$
$$\frac{(3+7)^2}{2((3)^2+(7)^2)}(1)+\frac{(3+8)^2}{2((3)^2+(8)^2)}(1)+\frac{(4+4)^2}{2((4)^2+(4)^2)}(2)+\frac{(4+5)^2}{2((4)^2+(5)^2)}(4)+\frac{(4+6)^2}{2((4)^2+(6)^2)}(2)+\frac{(4+7)^2}{2((4)^2+(7)^2)}(1)+$$
$$\frac{(4+9)^2}{2((4)^2+(9)^2)}(1)+\frac{(5+5)^2}{2((5)^2+(5)^2)}(2)+\frac{(5+6)^2}{2((5)^2+(6)^2)}(6)+\frac{(5+7)^2}{2((5)^2+(7)^2)}(1)+\frac{(5+8)^2}{2((5)^2+(8)^2)}(2)+\frac{(5+9)^2}{2((5)^2+(9)^2)}(1)+$$
$$\frac{(6+6)^2}{2((6)^2+(6)^2)}(1)+\frac{(6+7)^2}{2((6)^2+(7)^2)}(3)+\frac{(6+8)^2}{2((6)^2+(8)^2)}(1)+\frac{(7+7)^2}{2((7)^2+(7)^2)}(4)+\frac{(7+8)^2}{2((7)^2+(8)^2)}(1)+\frac{(7+9)^2}{2((7)^2+(9)^2)}(1)+$$
$$\frac{(8+8)^2}{2((8)^2+(8)^2)}(1)+\frac{(8+9)^2}{2((8)^2+(9)^2)}(2)+\frac{(9+9)^2}{2((9)^2+(9)^2)}(1)=83.84$$

j) $$\mathrm{CAI}(\zeta)=\sum\frac{2((du)^2+(dv)^2)}{(du+dv)^2}=\frac{2((1)^2+(2)^2)}{(1+2)^2}(2)+\frac{2((1)^2+(3)^2)}{(1+3)^2}(5)+\frac{2((1)^2+(4)^2)}{(1+4)^2}(2)+\frac{2((2)^2+(2)^2)}{(2+2)^2}(9)+$$
$$\frac{2((2)^2+(3)^2)}{(2+3)^2}(14)+\frac{2((2)^2+(4)^2)}{(2+4)^2}(6)+\frac{2((3)^2+(3)^2)}{(3+3)^2}(6)+\frac{2((3)^2+(4)^2)}{(3+4)^2}(2)+\frac{2((3)^2+(6)^2)}{(3+6)^2}(3)+$$
$$\frac{2((3)^2+(7)^2)}{(3+7)^2}(1)+\frac{2((3)^2+(8)^2)}{(3+8)^2}(1)+\frac{2((4)^2+(4)^2)}{(4+4)^2}(2)+\frac{2((4)^2+(5)^2)}{(4+5)^2}(4)+\frac{2((4)^2+(6)^2)}{(4+6)^2}(2)+$$
$$\frac{2((4)^2+(7)^2)}{(4+7)^2}(1)+\frac{2((4)^2+(9)^2)}{(4+9)^2}(1)+\frac{2((5)^2+(5)^2)}{(5+5)^2}(2)+\frac{2((5)^2+(6)^2)}{(5+6)^2}(6)+\frac{2((5)^2+(7)^2)}{(5+7)^2}(1)+$$
$$\frac{2((5)^2+(8)^2)}{(5+8)^2}(2)+\frac{2((5)^2+(9)^2)}{(5+9)^2}(1)+\frac{2((6)^2+(6)^2)}{(6+6)^2}(1)+\frac{2((6)^2+(7)^2)}{(6+7)^2}(3)+\frac{2((6)^2+(8)^2)}{(6+8)^2}(1)+$$
$$\frac{2((7)^2+(7)^2)}{(7+7)^2}(4)+\frac{2((7)^2+(8)^2)}{(7+8)^2}(1)+\frac{2((7)^2+(9)^2)}{(7+9)^2}(1)+\frac{2((8)^2+(8)^2)}{(8+8)^2}(1)+\frac{2((8)^2+(9)^2)}{(8+9)^2}(2)+$$
$$\frac{2((9)^2+(9)^2)}{(9+9)^2}(1)=92.84$$

Remdesivir's overall efficacy and great clinical applicability are indicated by its relatively high QGI(ζ) of 93.40 and CAI(ζ) of 92.84. Its strong quality is further supported by the CQI(ζ) of 90.24, which shows a noTable-positive influence. While the GQI(ζ) and ACI(ζ) values of 83.49 and 83.84, respectively, show slight areas for development in general quality and application, the QCI(ζ) of 85.84 indicates moderate quality. With considerable need for improvement in certain areas, Remdesivir's overall performance across these indices demonstrates its strong therapeutic potential, particularly in clinical settings.

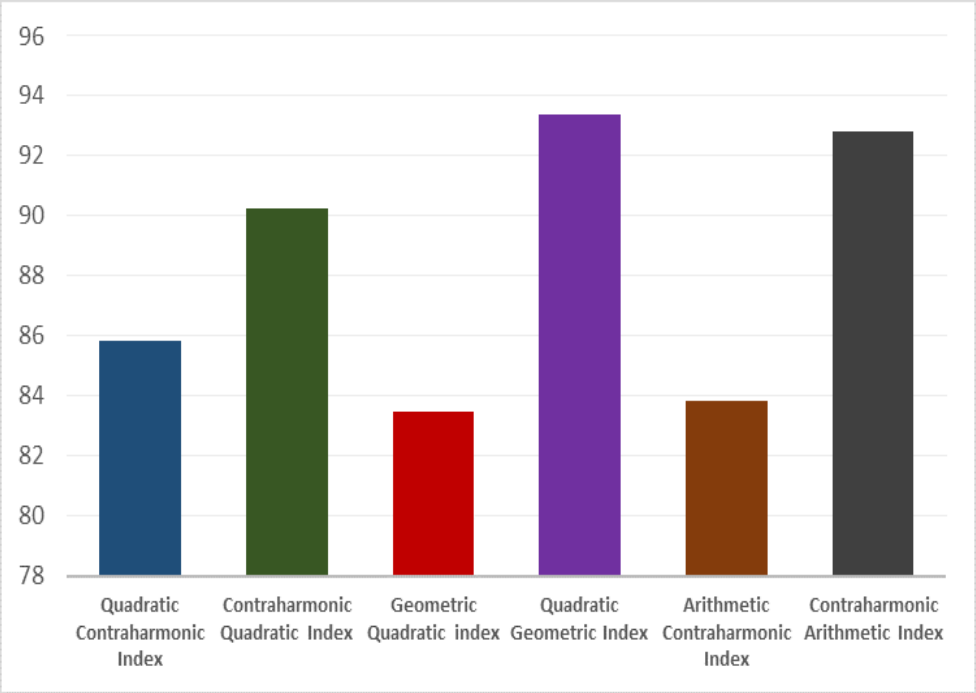

Figure-7: Comparative Analysis of Remdesivir

Theorem 2. The Quadratic-Contraharmonic Index (QCI), Contra Harmonic-Quadratic Index (CQI), Geometric Quadratic Index (GQI), Quadratic Geometric Index (QGI), Arithmetic Contraharmonic Index (ACI) And Contraharmonic Arithmetic index (CAI) for Chloroquine are as follow.

a) $\boldsymbol{NLQCI(\zeta) = 45.15}$
b) $\boldsymbol{CQI(\zeta) = 46.89}$
c) $\boldsymbol{GQI(\zeta) = 44.26}$
d) $\boldsymbol{QGI(\zeta) = 47.96}$
e) $\boldsymbol{ACI(\zeta) = 44.35}$
f) $\boldsymbol{CAI(\zeta) = 47.83}$

Proof. By using the degree-based edge partition of Table-2 and equations 1-6, we concluded these results.

Chloroquine's QGI(ζ) of 47.96 and CAI(ζ) of 47.83 indicate very moderate efficacy; its clinical applicability is indicated by the highest values. Although the CQI(ζ) of 46.89 indicates good quality, it is still below that of several other compounds. The overall performance is moderate, as shown by the QCI(ζ) value of 45.15. The ACI(ζ) and GQI(ζ) values of 44.26 and 44.35, respectively, point to areas that require further work, particularly in the areas of general quality and application. Although chloroquine has some beneficial effects overall, its effectiveness is inferior to that of more powerful medications, indicating areas that can use improvement.

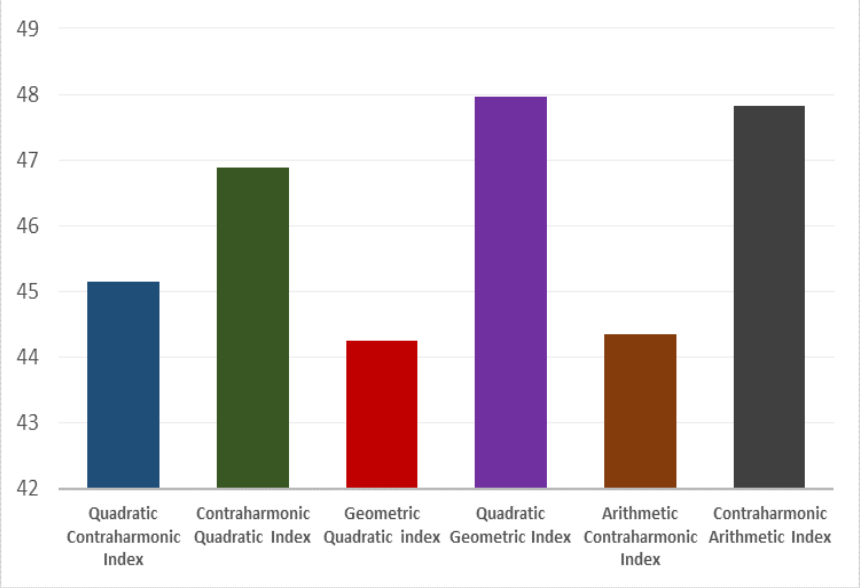

Figure-8: Comparative Analysis of Chloroquine

Theorem 3. The Quadratic-Contraharmonic Index (QCI), Contra Harmonic-Quadratic Index (CQI), Geometric Quadratic Index (GQI), Quadratic Geometric Index (QGI), Arithmetic Contraharmonic Index (ACI) And Contraharmonic Arithmetic index (CAI) for Hydroxychloroquine are as follows

a) $\mathbf{QCI}(\zeta) = \mathbf{47.17}$
b) $\mathbf{CQI}(\zeta) = \mathbf{48.87}$
c) $\boldsymbol{GQI}(\zeta) = \mathbf{46.29}$
d) $\boldsymbol{QGI}(\zeta) = \mathbf{49.92}$
e) $\mathbf{ACI}(\zeta) = \mathbf{46.38}$
f) $\mathbf{CAI}(\zeta) = \mathbf{49.79}$

Proof. By using the degree-based edge partition of Table-3 and equations 1-6, we concluded these results.

The relatively good clinical applicability of hydrochloroquine is indicated by its QGI(ζ) of 49.92 and CAI(ζ) of 49.79, which show favorable effects in these domains. While the QCI(ζ) of 47.17 stays within the moderate range, the CQI(ζ) value of 48.87 indicates respecTable-overall quality. Areas for possible improvement are indicated by the GQI(ζ) and ACI(ζ) values of 46.29 and 46.38, especially in general quality and application. In general, hydroxychloroquine exhibits steady performance; yet, its effectiveness seems to be moderate, with room for improvement in certain areas.

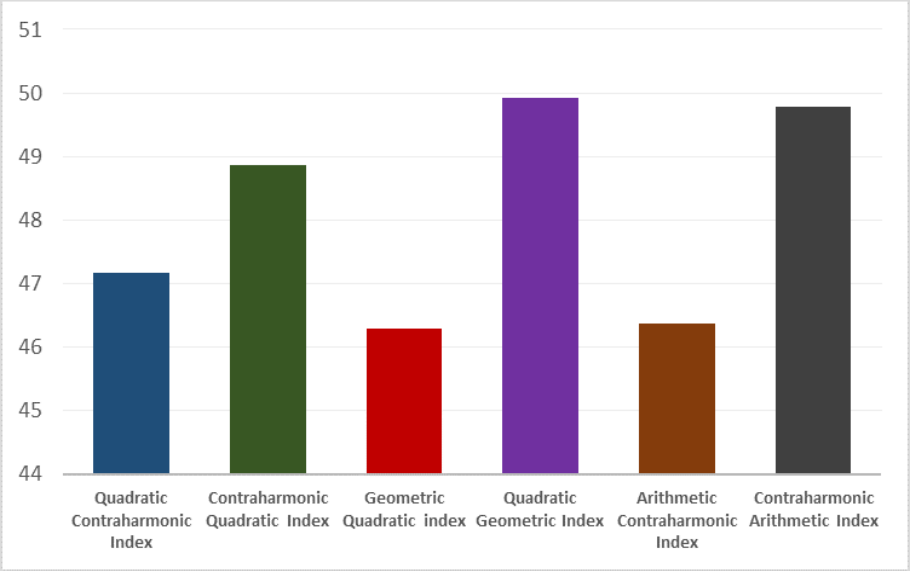

Figure-9: Comparative Analysis of Hydroxychloroquine

Theorem 4 The Quadratic-Contraharmonic Index (QCI), Contra Harmonic-Quadratic Index (CQI), Geometric Quadratic Index (GQI), Quadratic Geometric Index (QGI), Arithmetic Contraharmonic Index (ACI) And Contraharmonic Arithmetic index (CAI) for Theaflavin are as follows :

a) $\mathbf{QCI}(\zeta) = \mathbf{89.84}$
b) $\mathbf{CQI}(\zeta) = \mathbf{94.32}$
c) $\boldsymbol{GQI}(\zeta) = \mathbf{87.50}$
d) $\boldsymbol{QGI}(\zeta) = \mathbf{97.33}$
e) $\mathbf{ACI}(\zeta) = \mathbf{87.83}$
f) $\mathbf{CAI}(\zeta) = \mathbf{96.82}$

Proof. Similar proof by using the degree-based edge partition of Table-4 and equations 1-6 we computer the above results.

Theaflavin's remarkably high QGI(ζ) of 97.33 and CAI(ζ) of 96.82 indicate that it is highly efficacious and clinically applicable. Its exceptional quality is further supported by its CQI(ζ) of 94.32, which makes it a very promising chemical. While the GQI(ζ) and ACI(ζ) values of 87.50 and 87.83 show strong performance, but somewhat below the top scores, the QCI(ζ) of 89.84 shows strong overall quality. All things considered, theaflavin exhibits exceptional promise on a number of indices, with its clinical and general quality strengths highlighting its potent therapeutic qualities and effectiveness.

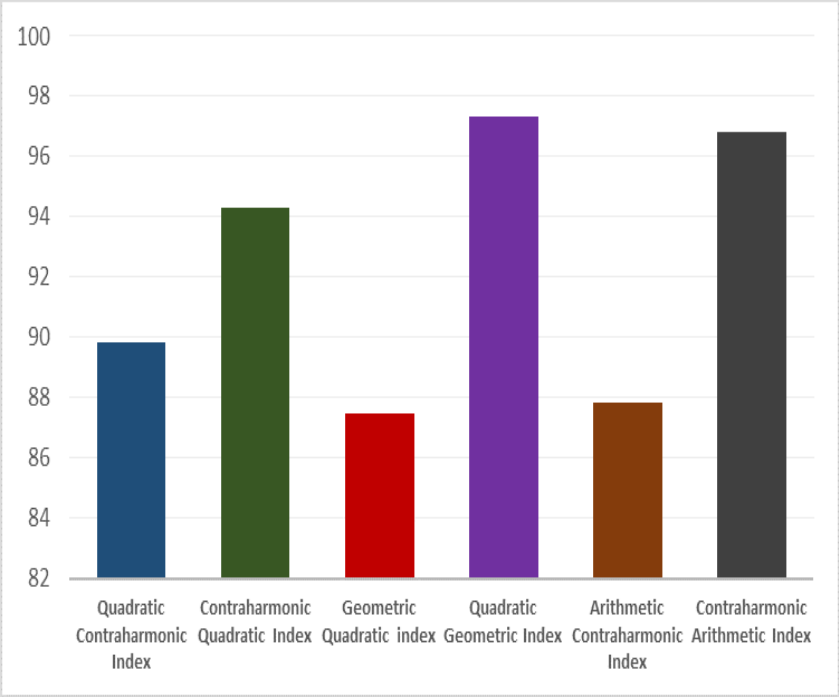

Figure-10 : Comparative Analysis of Theaflavin

Theorem 5: The Quadratic-Contraharmonic Index (QCI), Contra Harmonic-Quadratic Index(CQI), Geometric Quadratic Index (GQI), Quadratic Geometric Index (QGI), Arithmetic Contraharmonic Index (ACI) And Contraharmonic Arithmetic index (CAI) for Ritonavir are as follow.

a) $\mathbf{QCI(\zeta) = 104.02}$
b) $\mathbf{CQI(\zeta) = 108.12}$
c) $\boldsymbol{GQI(\zeta) = 101.88}$
d) $\boldsymbol{QGI(\zeta) = 110.83}$
e) $\mathbf{ACI(\zeta) = 102.16}$
f) $\mathbf{CAI(\zeta) = 110.40}$

Proof. By using the degree-based edge partition of Table-5 and equations 1-6, these results were computed.

Ritonavir performs excellently with an exceptional QGI(ζ) value of 110.83 and CAI(ζ) of 110.40, indicating outstanding clinical applicability and general quality. This is further supported by the CQI(ζ) value of 108.12, which speaks highly of the quality and effectiveness of Ritonavir. The QCI(ζ) equals 104.02, indicating strong overall quality, while GQI(ζ) equals 101.88 and ACI(ζ) equals 102.16, indicating high effectiveness and comparative consistency, with a slight variance. In general, the reports across all represent the compelling prowess and reliability of Ritonavir, which would thus constitute one of the most effective treatments often with higher rates of efficacies in various several aspects.

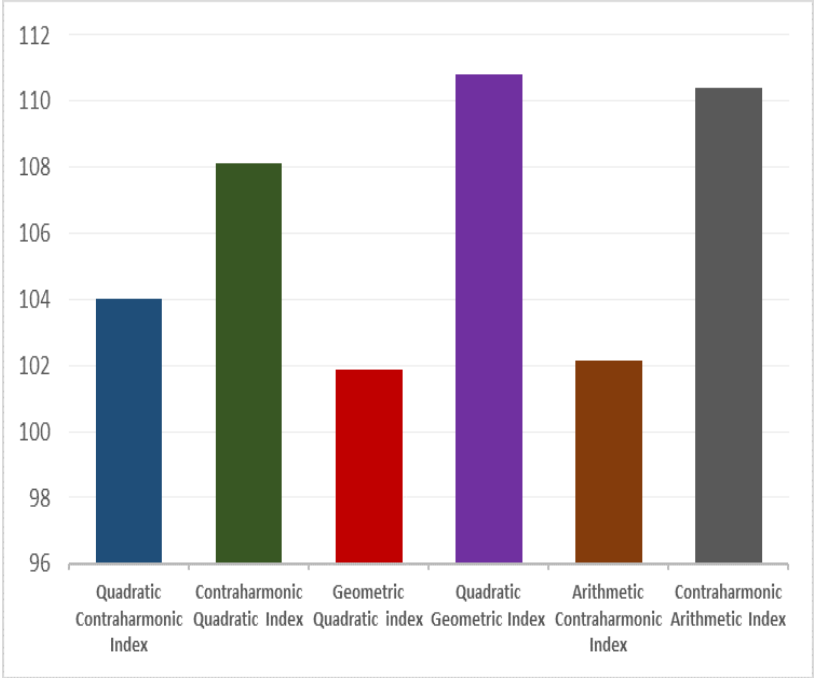

Figure-11: Comparative Analysis of Ritonavir

Theorem 6: The Quadratic-Contraharmonic Index (QCI), Contra Harmonic-Quadratic Index (CQI), Geometric Quadratic Index (GQI), Quadratic Geometric Index (QGI), Arithmetic Contraharmonic Index (ACI) And Contraharmonic Arithmetic index (CAI) for Arbidol are as follows:

a) $\mathbf{QCI}(\zeta) = \mathbf{60.70}$
b) $\mathbf{CQI}(\zeta) = \mathbf{63.40}$
c) $\boldsymbol{GQI}(\zeta) = \mathbf{59.28}$
d) $\boldsymbol{QGI}(\zeta) = \mathbf{65.23}$
e) $\mathbf{ACI}(\zeta) = \mathbf{59.49}$
f) $\mathbf{CAI}(\zeta) = \mathbf{64.92}$.

Proof. By using the degree-based edge partition of Table-6 and equations 1-6, we conclude these results.

The performance of Arbidol across the indices is moderate in efficacy, with some differential in the different areas. It has a maximum score, QGI(ζ), of 65.23, which indicates that this agent has fairly good outcomes in clinical applicability.QAI(ζ)-64.92 also exhibits quite commendable performance in the area of overall quality. CQI(ζ)-63.40 lends support to this premise with fair quality outcomes but the remaining indices, namely QCI(ζ)(60.70), ACI(ζ)(59.49),and GQI(ζ)(59.28), have lower scores, showing the areas needing improvement. Arbidol is consistent overall; however, the treatment cannot produce as high an effect as the more potent compounds.

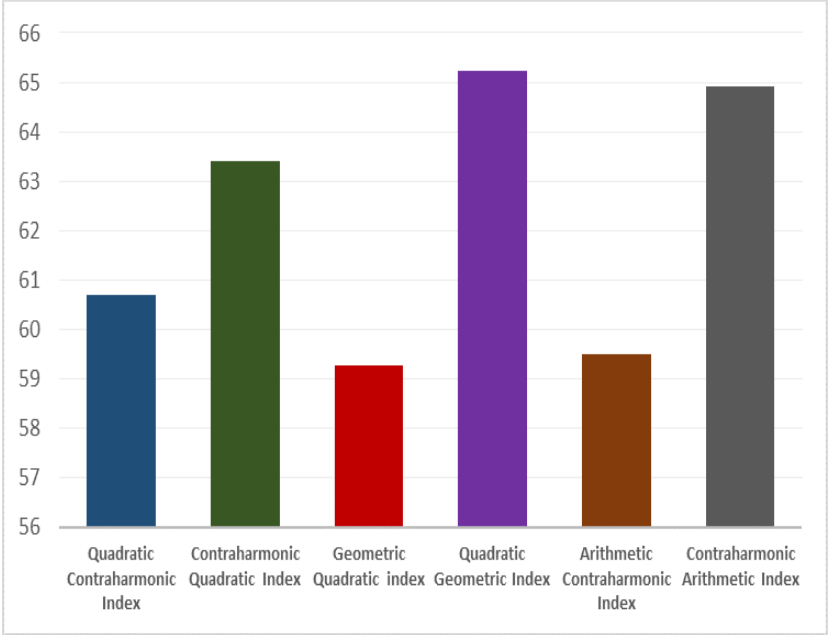

Figure-12. Comparative Analysis of Arbidol

4.2 Quantitative Structure Property Relationship (Qspr) Analysis Of Degree Based Topological Indices

This section aims to establish quantitative structure property relationships (QSPR) between topological indices and physicochemical properties of COVID-19 medications. Degree-based topological indices were used to model antiviral activity, boiling point, enthalpy of vaporization, flash point, molar refraction, polar surface area, and surface tension.

Table-7: Covid-19 Drugs And Their Physicochemical Properties

Drugs	Boiling Point (BP)	Enthalpy Of Vaporizartion (E)	Flash Point (Fp)	Molar Refractivity (MR)	Polar Surface Area (PSA)	Polarizability (P)	Surface Tension(T)	Molar Volume (MV)
REMDESIVIR	-	-	-	149.5	213	59.3	62.3	409
CHLOROQUINE	460.6	72.1	232.3	97.4	28	38.6	44.0	287.9
HYDROXYCHLOROQUINE	516.7	83.0	266.3	99.0	48	39.2	49.8	285.4
THEAFLAVIN	1003.9	153.5	336.5	137.3	218	54.4	138.6	301.0
RITONAVIR	947.0	144.4	526.6	198.9	202	78.9	53.7	581.7
ARBIDOL	591.8	91.5	311.7	121.9	80	48.3	45.3	347.3

Table-8: Values of Topological Indices for Molecular Graph Of Covid-19 Drugs

Drugs	QCI	CQI	GQI	QGI	ACI	CAI
REMDESIVIR	85.84	90.24	83.49	93.40	83.84	92.84
CHLOROQUINE	45.15	46.89	44.26	47.96	44.35	47.83
HYDROXYCHLOROQUINE	47.17	48.87	46.29	49.92	46.38	49.79
THEAFLAVIN	89.84	94.32	87.50	97.33	87.83	96.82
RITONAVIR	104.02	108.12	101.88	110.83	102.16	110.40
ARBIDOL	60.70	63.40	59.28	65.23	59.49	64.92

Table-9: Linear Regression Model's Correlation Coefficient (r)

INDICES	BP	E	Fp	MR	PSA	P	T	MV
QCI	0.9602	0.9559	0.9017	0.9355	0.9528	0.9353	0.4665	0.7597
CQI	0.9634	0.9591	0.8958	0.9303	0.9574	0.9302	0.4750	0.7510
GQI	0.9583	0.9540	0.9049	0.9383	0.9498	0.9381	0.4618	0.7646
QGI	0.9654	0.9611	0.8918	0.9266	0.9608	0.9264	0.4799	0.7449
ACI	0.9587	0.9544	0.9043	0.9378	0.9504	0.9376	0.4626	0.7637
CAI	0.9650	0.9607	0.8926	0.9274	0.9601	0.9272	0.4789	0.7462

4.3 Discussions

The calculated degree-based topological indices give quantitative information on the structural complexity and connectivity of the selected drug molecules related to COVID-19. At all aspects, Ritonavir gave the highest value followed by Theaflavin and Remdesivir while Chloroquine and Hydroxychloroquine had the lowest value in all aspects. The ranking would indicate that Ritonavir has a more complex molecular graph with higher vertex-degree interactions, deeper bonding structure, and density. The ranking will suggest that Ritonavir has more complex molecular graph with better vertex-degree interactions, more bonding structure and density. By comparison, the lower values for both the molecular connectivity descriptors, Chloroquine and Hydroxychloroquine, have simpler molecular connectivity. Structurally, the higher index values, observed for Ritonavir and Theaflavin are due to the presence of high number of multiple functional groups and bigger molecular frameworks. For this molecular complexity is significant since it can affect the physicochemical behavior, such as molecular polarizability, refractivity, and interaction potential. The remarkably high values of the descriptors also were observed with remdesivir, which have a structurally complex nucleotide-analogue framework. Arbidol was in between, showing moderate molecular complexity relative to the other molecules.

The QSPR correlation analysis also shows that the proposed indices are strongly correlated with a number of physicochemical properties such as boiling point, enthalpy of vaporization, molar refractivity, polar surface area, and the polarizability. This indicates that descriptors chosen are able to represent size-, branching-, and connectivity-related aspects of molecules. The good correlation with molar refractivity, in particular, and with polarizability is particularly noteworthy because these properties are related to molecular volume and electron distribution. Likewise, based on the correlation with the polar surface area, polar heteroatoms and functional groups might be expected to have some correlation with these indices. But the conclusions drawn from the findings should be taken with a grain of salt. There is no correlation

between the topological index values and the antiviral activity or therapeutic action. These for the most part refer to increased graph-based structural complexity. Further properties of the biological activity include conformational change, target binding affinity, solubility, pharmacokinetics, metabolic stability and toxicity. Thus, the present findings encourage the use of indices based on degrees as initial mathematical indicators, but drug efficacy cannot be established based on such indices alone.

Another important observation made was that surface tension correlated with the selected indices comparatively less. It means that the degree-based connectivity cannot fully explain some physicochemical properties. The properties of such substances might rely more on three-dimensional shape, intermolecular forces, hydrogen bonding and electronic interactions. Thus, proposed descriptors are beneficial but need to be used in association with other molecular descriptors for a better QSPR prediction. Overall, the results indicate that degree-based topological indices have the potential of effectively discriminating between the selected drugs based on the complexity of the molecular graph and correlating to a number of physicochemical properties. However, this study should be presented as a computational and mathematical appraisal, not a direct evaluation of antiviral activity.

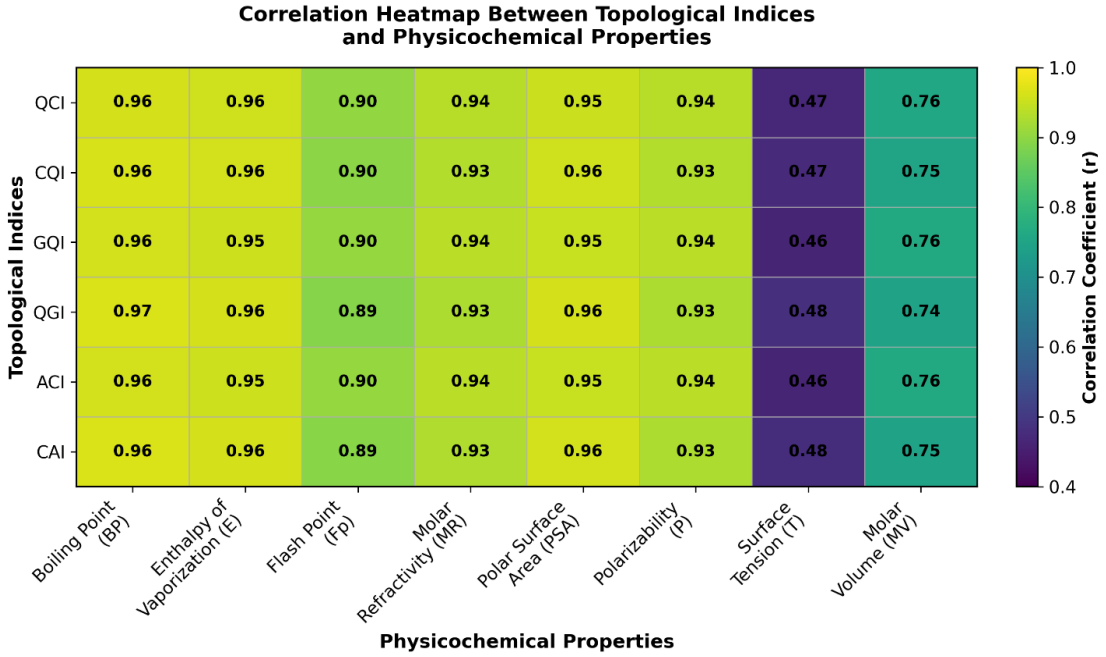

All degree-based topological indices are strongly correlated with most of the physicochemical properties (Figure 13), particularly with the boiling point, enthalpy of vaporization, flash point, molar refractivity, polar surface area and polarizability. The highest correlation is obtained for QGI and CAI indicating that these indices are helpful in representing the molecular connectivity and structural complexity that are associated with the properties related to size, polarity and energy. The matrix also presents some significant weaknesses, however. There are insignificant correlations between surface tension and all the indices, which suggests that this property is not sufficiently represented by the degree-based connectivity and may be more dependent on the 3D geometric structure, intermolecular forces and hydrogen bonding. Partially, weakly correlated with molar volume, indicating some but incomplete structural representation. In conclusion, the usefulness of these indices for physicochemical prediction

using QSAR as a study example is confirmed from the heatmap distributed, but the similarity of the correlational pattern with all the descriptors studied makes it possible to suggest about their redundancy. Thus, more comprehensive and larger data sets, as well as the use of more 3D/electronic descriptors, should be introduced working with them before predicting new properties or pharmacological applications.

4.4 Limitation of the Study

There are a number of limitations in this study. First, the analysis involves limited compounds (only six), and this results in less power and reliability of the QSPR findings. Second, only degree-based topological descriptors were utilized, which means that the geometry and stereochemistry, electronic distribution and conformational flexibility of the molecules were not taken into account. Thirdly, a QSPR analysis method relies on correlations and correlations do not imply predictive reliability or causality. Fourth, other biological activity parameters such as IC50, EC50, binding affinity, toxicity, and ADMET properties were not considered. Thus, conclusions about the antiviral activity of the product should not be drawn from the results. Lastly, the lack of external validation and cross validation restricts the strength of the proposed QSPR models.

5.0 Conclusion

The purpose of this study is to reveal how useful the degree-based topological indices are in structural characterization and in the analysis of the structural activity of selected antiviral compounds included in a series of compounds associated with COVID-19. The degree-based edge partitioning of Molecular graph has been used to compute six descriptors of Remdesivir, CQI, Hydroxychloroquine, GQI, QGI, ACI and CAI. This variation is clearly seen with the compounds, with Ritonavir giving the highest scores in all the calculated indices, followed by Theaflavin and Remdesivir. These higher descriptor values indicate their higher structural complexity and better topological representation in comparison with Arbidol, Hydroxychloroquine and Chloroquine. The QSPR analysis also supports this, by demonstrating that the suggested indices have high correlation with a number of important physicochemical properties. Co-ordinates were obtained with high correlation coefficient for boiling point, enthalpy of vaporization, flash point, molar refractivity, polar surface area and polarizability parameters in particular. The indices were significantly correlated with each other (ranging 0.92 to 0.98); QGI, CAI exhibited especially high correlations with boiling point, enthalpy of vaporization and polar surface area, as they might have a good predictive value toward the selected molecular properties. Unfortunately, the correlation with surface tension is less strong and molar volume is less strongly associated with the indices chosen, suggesting that not all physicochemical properties can be as closely predicted by the selected indices. Overall, the results suggest that the calculated topological descriptors could be useful mathematical tools for screening some viable antiviral drug candidates in the initial stages of the computational process. Results indicated that Ritonavir, Theaflavin, and Remdesivir are structurally significant while based on calculated descriptors; these results should be understood as molecular insights based on descriptors and not on actual clinical data for antiviral efficacy. Future work could involve testing the proposed method with more extensive antiviral libraries, more molecular descriptors, machine-learning generated QSPR models, and experimental data to test the reliability and applicability of the proposed method in the field of drug discovery.

Acknowledgment

The authors also extend their appreciation to the funding bodies, academic institutions or other contributors that have supported this research. Additional acknowledgment goes also to Superior University for providing useful feedback and recommendation throughout the study.

Conflict of Interest

This work also has no conflict of interest to the authors.

REFERENCES

[1] Kirmani, S. A. K., Ali, P., and Azam, F. 2021. Topological indices and QSPR/QSAR analysis of some antiviral drugs being investigated for the treatment of COVID-19 patients. International Journal of Quantum Chemistry, 121(9), p.e26594.

[2] Ismael, M., Zaman, S., Elahi, K., Koam, A. N., and Bashir, A. 2024. Analytical expressions and structural characterization of some molecular models through degree-based topological indices. Mathematical Modelling of Engineering Problems, 11(1), pp.101-145.

[3] Bhatia, K. S., Gupta, A. K., and Saxena, A. K. 2023. Physicochemical significance of topological indices: Importance in drug discovery research. Current Topics in Medicinal Chemistry, 23(29), pp.2735-2742.

[4] Arockiaraj, M., Greeni, A. B., and Kalaam, A. A. 2024. Comparative analysis of reverse degree and entropy topological indices for drug molecules in blood cancer treatment through QSPR regression models. Polycyclic Aromatic Compounds, 44(9), pp.6024-6041.

[5] Banerjee, A., Kar, S., Roy, K., Patlewicz, G., Charest, N., Benfenati, E., and Cronin, M. T. 2024. Molecular similarity in chemical informatics and predictive toxicity modeling: From quantitative read-across (q-RA) to quantitative read-across structure–activity relationship (q-RASAR) with the application of machine learning. Critical Reviews in Toxicology, 54(9), pp.659-684.

[6] Raza, A., Ismaeel, M., and Tolasa, F. T. 2024. Valency-based novel quantitative structure-property relationship (QSPR) approach for predicting physical properties of polycyclic chemical compounds. Scientific Reports, 14(1), p.7080.

[7] Hakeem, A., Ullah, A., Zaman, S., Hamed, Y. S., and Belay, M. B. 2024. Computational insights into flavonoid molecular structures and their QSPR modeling via degree-based molecular descriptors. Chemical Papers, pp.1-16.

[8] Havare, Ö. Ç. 2022. Quantitative structure analysis of some molecules in drugs used in the treatment of COVID-19 with topological indices. Polycyclic Aromatic Compounds, 42(8), pp.5249-5260.

[9] Kansal, N., Garg, P., and Singh, O. 2023. Temperature-based topological indices and QSPR analysis of COVID-19 drugs. Polycyclic Aromatic Compounds, 43(5), pp.4148-4169.

[10] Alghamdi, A. M., Hamid, K., Iqbal, M. W., Ashraf, M. U., Alshahrani, A., and Alshamrani, A. 2023. Topological evaluation of certain computer networks by contraharmonic-quadratic indices. Computers, Materials & Continua, 74(2), pp.145-189.

[11] Das, S., Rai, S., and Kumar, V. 2024. On topological indices of Molnupiravir and its QSPR modelling with some other antiviral drugs to treat COVID-19 patients. Journal of Mathematical Chemistry, 62(10), pp.2581-2624.

[12] Aslam, K., Ali, M., Hashmi, M. U., Ahamd, A., and Ahmad, U. 2024. Calculating topological indices of Benes and Butterfly Network. Journal of Computing & Biomedical Informatics, 8(01).

[13] Cherifi, H., Palla, G., Szymanski, B. K., and Lu, X. 2019. On community structure in complex networks: challenges and opportunities. Applied Network Science, 4(1), pp.1-35.

[14] Sivakumar, B., Rajkumar, V., and Siddiqui, M. K. 2024. Quantifying algebraic connectivity: Sombor index and polynomial in some graphs of commutative ring Z p. Symmetry, 16(12), p.1615.

[15] Zhang, Y., Khalid, A., Siddiqui, M. K., Rehman, H., Ishtiaq, M., and Cancan, M. 2023. On analysis of temperature-based topological indices of some COVID-19 drugs. Polycyclic Aromatic Compounds, 43(4), pp.3810-3826.

[16] Nagarajan, S., Priyadharsini, G., and Pattabiraman, K. 2023. QSPR modeling of status-based topological indices with COVID-19 drugs. Polycyclic Aromatic Compounds, 43(8), pp.6868-6887.